

Geochemical Sources of Energy for Microbial Metabolism in Hydrothermal Ecosystems: Obsidian Pool, Yellowstone National Park



Everett L. Shock^{1,2,*} | Melanie Holland¹ | D'Arcy R. Meyer-Dombard³ | Jan P. Amend³

¹Department of Geological Sciences, Arizona State University, Tempe

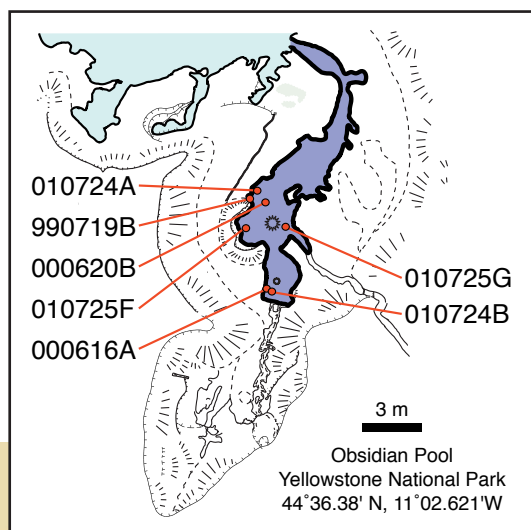
²Department of Chemistry & Biochemistry, Arizona State University, Tempe

³Department of Earth & Planetary Sciences, Washington University, St. Louis, MO

**Corresponding Author:*

Dept of Geological Sciences, Box 871404
Arizona State University, Tempe, AZ 85287

Phone: 480.965.0631 Fax: 480.965.8102 Email: eshock@asu.edu



ABSTRACT

Potential sources of metabolic chemical energy that thermophiles can use in a hot spring ecosystem can be quantified by combining analytical and thermodynamic data, as in this case for Obsidian Pool at Yellowstone National Park. This hot spring is chosen because of extensive previous efforts to characterize its microbial community structure with molecular methods, as well as successful efforts to isolate microorganisms from the pool and study their physiology. We quantify the potential metabolic energy available from 182 reactions that are out of equilibrium in Obsidian Pool, rank the sources by energy availability, and categorize the resulting energy structure by electron acceptor. The results provide the first comprehensive view of the distribution of energy supplies from chemical reactions in a hot spring ecosystem. Hypotheses derived from these results can be tested through experiments on the relative rates of proposed metabolic processes, genomic and proteomic analyses of natural samples, and informed efforts to isolate and study novel organisms.

Key Words

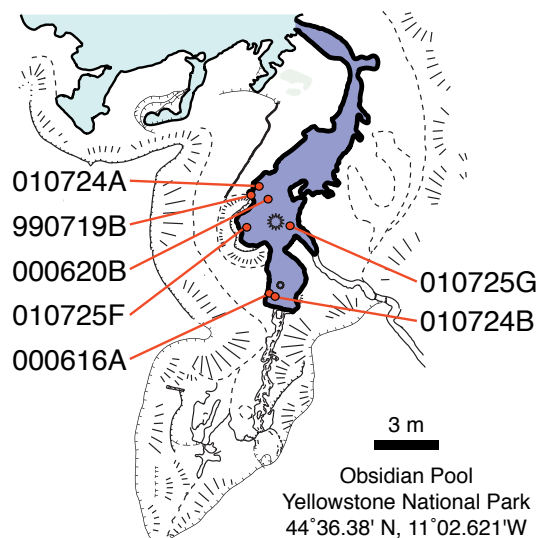
energy sources
gas composition
geochemical data
metabolism
Obsidian Pool
thermodynamic analysis

1.0 INTRODUCTION

Biology and geochemistry are linked through the biological mediation of reactions involving geological materials. This linkage is acute in hot spring ecosystems where photosynthesis does not occur ($\geq 75^{\circ}\text{C}$ at Yellowstone; Brock 1978; Cox and Shock 2003) and the entire microbial community depends on chemical sources of energy. Although the presence of non-photosynthetic microorganisms at the highest temperatures of Yellowstone hot springs was documented more than a century ago (Setchell 1903; see also Reysenbach and Shock 2002), progress in identifying the geochemical sources of energy that support these organisms has been sluggish. This may be related to why only a handful of high-temperature organisms from beyond the photosynthetic fringe at Yellowstone are in culture where their physiology and metabolism can be studied. At the same time, considerable progress has been made using molecular methods to obtain genetic characterizations of microbial communities in hot springs. One of the best studied systems from this perspective is Obsidian Pool.

2.0 THE SETTING

Obsidian Pool (**Figure 1**) is a persistent hot spring south of Goose Lake in the Mud Volcano Area, which is located to the southwest of the Sour Creek resurgent dome within the Yellowstone Caldera (Christiansen 2001). Though the pool is relatively shallow (10–100 cm) and varies in size somewhat from year to year (see **Figure 2, next page**), our time series of measurements (see below) shows that the pool temperature and pH are relatively constant at $78.9^{\circ}\text{C} \pm 4.0^{\circ}$ and $6.7 \text{ pH} \pm 0.4$, respectively (90% confidence intervals). Fluid flows slowly from Obsidian Pool to the larger hot spring to the north. The Mud Volcano Area in general and Obsidian Pool in particular show inputs of magmatic gases, including carbon dioxide, hydrogen, and hydrogen sulfide (Werner et al. 2000). Obsidian Pool is named for the black, sandy material covering the bottom of the pool. This material is volcanic glass with a grain size of 0.1 to 2 mm coated in a material that may be pyrite (Barns et al. 1994; Burggraf et al. 2001). As described here, the pool has ample sources of energy for chemoautotrophic



↑ **Figure 1.** Map of Obsidian Pool (north at top) showing the relation between Obsidian Pool (darker blue) and the larger hot spring (lighter blue) it flows into, as well as sample locations (mapping by Bob Osburn). Sample numbers reflect the date that each sample was taken in year-month-day notation. Splayed hachures indicate descending slopes to the springs from the surrounding meadow, and main gas sources are indicated in the central and southern areas of the hot spring. Dark outline of Obsidian Pool indicates the water edge in 1999. Water levels change with time, as suggested by the pictures in Figure 2.

microorganisms and, along with sites like Octopus Spring and Nymph Creek, has become a focus for microbiological work in Yellowstone (Barns et al. 1994, 1996; Burggraf et al. 1997, 2001; Fishbain et al. 2003; Graber et al. 2001; Huber et al. 1995, 1998; Hugenholtz et al. 1998; Kashefi et al. 2002; Roychoudhury 2004).

3.0 OBSIDIAN POOL MICROBIOLOGY

Obsidian Pool has been the site of phylogenetic studies, culturing efforts, and biological rate measurements. Published 16S rRNA clone libraries derived from Obsidian Pool samples show an incredible diversity of organisms inhabiting the hot spring environment. A bacterial clone library created from a stromatolite-like sample taken in 1993 contained more than 50 unique and uncultured phenotypes distributed among 14 bacterial divisions, as well as

12 groups of cloned sequences that were phylogenetically distant from known bacterial divisions (Hugenholtz et al. 1998). An archaeal clone library constructed from the same sample was described as showing “remarkable diversity” with its 12 phylotypes, 11 of which are distributed within the Crenarchaeota, and the twelfth representing the deeply branching Korarchaeota (Barns et al. 1994). Another archaeal library from Obsidian Pool created by some of the same authors (which may or may not have been constructed from the same original sample; Barns et al. 1996) contained five sequences that overlapped with those reported in the 1994 paper, including a second detection of the Korarchaeota, as well as 19 new sequences within the Crenarchaeota.

These clone libraries should provide an overview of the potentially active organisms in the pool, though most of the organisms corresponding to the sequenced clones are as yet unknown. While inference of physiology from phylogeny is inherently biased, a few of the clades represented in the Obsidian Pool trees exhibit some metabolic coherence. These groups include two bacterial divisions—Aquificales, whose members oxidize hydrogen, sulfur, and thiosulfate; and a mainly sulfate-reducing subset of the delta-Proteobacteria—as well as four genera: *Archaeoglobus*, containing sulfate-reducing archaea; *Pyrobaculum*, which contains microaerophilic and nitrate-reducing archaea; *Thermofilum*, containing heterotrophic anaerobic sulfur-respiring archaea; and *Thermus*, containing organotrophic bacteria. Inferences like these can form a basis for enrichment cultures targeted at specific metabolisms.

The two well-characterized microorganisms from Obsidian Pool can be related to the phylogenetic analyses. *Thermosphaera aggregans* (Huber et al. 1998) is a fermentative heterotroph that was plucked from



↑ **Figure 2.** Two views of Obsidian Pool from the southern end: left, during July 1999 when originally mapped; right, during July 2004 when water level was considerably higher. Dark material surrounding parts of the pool contains sand-sized particles of volcanic glass. Bubbles result from release of gas through the hot spring, which is not hot enough to boil.

a primary enrichment using optical tweezers (Huber et al. 1995; Burggraf et al. 2001), and is closely related to a cloned sequence (pSL91) from Obsidian Pool. *Geothermobacterium ferrireducens* (Kashefi et al. 2002) is an iron reducer that is closely related to Obsidian Pool clones within the delta-Proteobacteria that had been envisioned as sulfate-reducing organisms based on close relatives. *G. ferrireducens* has a strict metabolism and, out of the 37 electron donors and 20 electron acceptors tested, will only reduce poorly-crystalline iron oxides with hydrogen. It did not reduce sulfate under any of the conditions tested, which suggests the need for re-evaluating the potential metabolism of other Obsidian Pool phylotypes in the delta-Proteobacteria.

Though the delta-Proteobacteria in the Obsidian Pool library may not be sulfate reducers, biologically mediated sulfate reduction does occur in the Obsidian Pool environment (the electron donor for this reaction is not identified). Fishbain et al. (2003) measured rates of sulfate reduction at Obsidian Pool in ^{35}S -sulfate core injection experiments and attempted enrichment cultures of sulfate-reducers, with no success. Also at Obsidian Pool, Roychoudhury (2004) measured both “natural” (unsupplemented) sulfate reduction rates and rates of sulfate reduction with added organic substrates, though the addition of organic substrates did not increase the rate.

The rates that Roychoudhury measured were a factor of five lower than those obtained by Fishbain et al. One sulfate-reducing organism has been cultured from Obsidian Pool, described by Burggraf et al. (2001) as an *Archaeoglobus* sp. that reduces sulfate (no mention of the electron donor). This organism, like *T. aggregans*, was isolated using optical tweezers and is closely related to an environmental sequence in the archaeal clonal libraries (Barns et al. 1994, 1996).

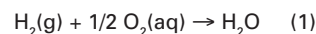
Taken together, phylogenetic and physiological data suggest that hydrogen oxidation, sulfur oxidation, nitrate reduction, ferric oxide reduction, and sulfate reduction all provide energy for microbial metabolism in Obsidian Pool. The purpose of this paper is to assess the availability of energy from an independent geochemical perspective, and provide the framework for linking biological and geochemical processes in hydrothermal ecosystems.

4.0 GEOCHEMICAL ENERGETICS AT OBSIDIAN POOL

Equilibrium is the lowest energetic state of a geochemical system; therefore, when chemical constituents of a system are not in equilibrium there is the potential for reactions to occur. At constant temperature and pressure, the driving force for reactions to proceed is the minimization of the overall Gibbs energy of the system. Evaluating the Gibbs energy of a system, and therefore determining which reactions can take place, starts with an analysis of the equilibrium state of the chemical system at constant temperature and pressure. The extent to which the real system differs from the equilibrium state can be related directly to the potential for various reactions to occur, and thus to the quantifiable geochemical energy in the system. Chemoautotrophic microorganisms obtain energy from chemical systems by catalyzing electron transfer reactions (oxidation-reduction reactions) that are out of equilibrium. By definition, these disequilibria are thermodynamically favored but kinetically inhibited reactions, and life (through the catalytic action of enzymes) provides an alternative pathway for these reactions, circumventing the kinetic barriers. Most of the oxidation-reduction reactions that support life involve the elements hydrogen, oxygen,

nitrogen, carbon, sulfur, iron, and manganese (Amend and Shock 2001).

As an example, it is possible that members of Aquificales, which appear in several clone libraries from in and around Obsidian Pool (Hugenholz et al. 1998; Graber et al. 2001; Spear et al. this volume; Meyer-Dombard et al. submitted), gain energy from hydrogen oxidation, which can be written as



where (g) designates that hydrogen is in the gas phase, and (aq) indicates that oxygen is dissolved in the aqueous solution of the hot spring. (This version of the reaction is readily related to our analytical data: H_2 from gas samples and dissolved O_2 measured in the field.) The amount of energy that can be released from reaction (1) can be evaluated by comparing the equilibrium state with the natural state, which, with measurable levels of both oxygen and hydrogen, is far from equilibrium. It is convenient to do this with the chemical affinity of each reaction (A), which is defined as the partial derivative of the overall Gibbs energy with respect to the progress of each reaction at constant temperature and pressure. Like the overall Gibbs energy, the chemical affinity is equal to zero at equilibrium, and has either positive or negative values if the natural system is out of equilibrium. By convention, positive values of A indicate situations where energy would be released if the reaction were to proceed in the direction that it is written.

The chemical affinity of a reaction (r) is given by

$$A = RT \ln K_R/Q_R \quad (2)$$

where R represents the gas constant, T stands for temperature, K_R stands for the equilibrium constant for the reaction, and the activity product (Q_R) is given by

$$Q_R = \prod a_i^{v_{i,R}} \quad (3)$$

where a_i stands for the activity of the *ith* constituent of the reaction, and $v_{i,R}$ represents the stoichiometric reaction coefficient, which is negative for reactants and positive for products.

In the case of reaction (1),

$$Q_1 = [a \text{H}_2\text{O}] / [a \text{H}_2(\text{g})][a \text{O}_2(\text{aq})]^{1/2} \quad (4)$$

the equilibrium constant is related to the standard state Gibbs energy (ΔG_R°) by

$$RT \ln K_R = -\Delta G_R^\circ \quad (5)$$

and depends only on the temperature and pressure of the natural system and not on its composition. In contrast, evaluating the activity product requires analytical data for concentrations from the natural system, together with the means to calculate activities from concentrations. The latter is easily accomplished with versions of the extended Debye-Hückel equation for activity coefficients (see below), and the former are obtained through field and laboratory analyses.

To evaluate the amount of energy available from reaction (1) at Obsidian Pool, we need the hot spring temperature to calculate the appropriate value of the equilibrium constant. We also need to know concentrations of $\text{H}_2(\text{g})$, $\text{O}_2(\text{aq})$, and major ion concentrations to calculate the ionic strength of the solution; obtain activities of $\text{H}_2(\text{g})$, $\text{O}_2(\text{aq})$, and H_2O ; and evaluate Q_1 . It is then possible to

solve equation (2) for the chemical affinity for reaction (1), which will be positive if energy is available.

As a result of field work at Obsidian Pool since 1999 (see description of analytical methods below), we have several sets of measurements that yield values of A for reaction (1). The average of these values is $99.3 \pm 3.7 \text{ kJ/mol e}^-$ (90% confidence interval) and the small range of values reveals that conditions at Obsidian Pool vary over relatively small ranges of temperature, ionic strength, and dissolved gas concentrations. This means that Obsidian Pool is far from behaving as a closed system, and that it can be thought of as a natural chemostat for the hydrogen oxidation reaction. Determining whether Obsidian Pool also acts like a natural chemostat for other energy-yielding reactions, and how the amount of energy from hydrogen oxidation compares with other energy-yielding chemical reactions, can be accomplished with analytical data and a thermodynamic analysis of the overall state of disequilibria in the system.

5.0 GEOCHEMICAL ANALYSES

Water, gas, and sediment samples from Obsidian Pool were obtained during field work from 1999-2001. Analytical data for these samples were collected in the field and

Table 1. Analytical data on water samples from Obsidian pool. Sample numbers encode the date that the sample was taken in year-month-day order. Spectrophotometric measurements of dissolved oxygen (DO), nitrate, nitrite, total sulfide (ΣS^{2-}), total ammonia (ΣNH_3), aqueous silica, and ferrous iron were made in the field and are reported here in μM (bdl = below detection limit, --- = not measured). Alkalinity (alk) by titration in the field is reported in mg/kg as CaCO_3 . Major anion and cation data were obtained by ion chromatography in the lab and are reported in μM .

| Sample# | T, °C | pH | Con. | DO | NO_3^- | NO_2^- | ΣS^{2-} | ΣNH_3 | SiO_2 | Fe^{2+} | alk | F ⁻ | Cl ⁻ | Br ⁻ | SO_4^{2-} | Na^+ | K^+ | Mg^{2+} | Ca^{2+} |
|---------|-------|------|-------|------|-----------------|-----------------|-----------------------|---------------------|----------------|------------------|------|----------------|-----------------|-----------------|--------------------|---------------|--------------|------------------|------------------|
| 990719B | 77.2 | 6.48 | 670. | 69.1 | 31. | 1.3 | 1.8 | 20. | --- | 0.54 | 134. | 305. | 522. | bdl | 702. | 2997. | 609. | 395. | 556. |
| 000616A | 80.9 | 6.64 | 1076. | 37.5 | 35. | 0.89 | bdl | 5.9 | 2730. | 0.54 | 165. | 316. | 440. | bdl | 294. | 2094. | 491. | 458. | 563. |
| 000620B | 81.4 | 6.78 | 324. | 56.3 | bdl | 0.09 | 2.8 | 21. | 3150. | 0.54 | 120. | 346. | 418. | bdl | 389. | 1725. | 375. | 340. | 419. |
| 010724A | 78.7 | 6.4 | 620. | 31.3 | bdl | 3.0 | 1.8 | 16. | 1360. | bdl | 120. | 347. | 604. | 9.6 | 579. | 2367. | 529. | 411. | 569. |
| 010724B | 78.6 | 6.5 | 750. | 81.3 | 1.6 | 3.0 | 1.8 | 12. | 3310. | 0.18 | 148. | 350. | 606. | 2.3 | 331. | 2353. | 541. | 414. | 560. |
| 010725F | 79.9 | 7.0 | 655. | 18.8 | 1.6 | 2.6 | 1.7 | 21. | 1810. | bdl | 121. | 351. | 601. | 9.5 | 566. | 2379. | 541. | 409. | 556. |
| 010725G | 75.8 | 6.8 | 1005. | 18.3 | 13. | 3.0 | 2.2 | bdl | 4080. | 0.36 | 156. | 341. | 621. | bdl | 315. | 1568. | 352. | 274. | 369. |

Table 2. Mole fractions of gases in samples of gas collected from Obsidian Pool, together with field measurements of temperature, pH, and conductivity. Samples are a subset of those listed in Table 1.

| Sample | T°C | pH | cond(μ S) | CO ₂ | H ₂ S | He | H ₂ | Ar | O ₂ | N ₂ | CH ₄ | CO |
|---------|------|------|----------------|-----------------|------------------|-----------------------|-----------------------|-----------------------|-----------------------|-----------------------|-----------------------|-----------------------|
| 000616A | 80.9 | 6.64 | 1076. | 0.962 | 0.0322 | 1.29×10 ⁻⁴ | bdl | 8.61×10 ⁻⁵ | bdl | 4.84×10 ⁻³ | 3.75×10 ⁻⁴ | 6.23×10 ⁻⁷ |
| 000620B | 81.4 | 6.78 | 324. | 0.955 | 0.0425 | 1.36×10 ⁻⁵ | 6.33×10 ⁻⁴ | 2.52×10 ⁻⁵ | bdl | 1.81×10 ⁻³ | 1.96×10 ⁻⁴ | 1.60×10 ⁻⁷ |
| 010724A | 78.7 | 6.4 | 620. | 0.985 | 0.0144 | 1.21×10 ⁻⁶ | 5.50×10 ⁻⁵ | 2.50×10 ⁻⁶ | 4.10×10 ⁻⁷ | 1.99×10 ⁻⁴ | 2.15×10 ⁻⁵ | 1.21×10 ⁻⁷ |
| 010724B | 78.6 | 6.5 | 750. | 0.975 | 0.0234 | 2.35×10 ⁻⁶ | 1.19×10 ⁻⁴ | 1.64×10 ⁻⁵ | 3.19×10 ⁻⁵ | 1.09×10 ⁻³ | 4.73×10 ⁻⁵ | bdl |

subsequently in the laboratory. Field measurements included temperature, pH, conductivity, alkalinity, and concentrations of dissolved oxygen, nitrate, nitrite, total ammonia, ferrous iron, total sulfide, and dissolved silica. Results are summarized in **Table 1**. Laboratory measurements of major cations and anions are also listed in **Table 1**, and analyses from gas samples are listed in **Table 2**.

Temperature, pH, and conductivity in μ S were measured with handheld meters that are easily recalibrated in the field (YSI 30 and Orion 290A+ meters, which operate up to 100°C). Alkalinity was determined in the field by titration with sulfuric acid using colorimetric indicators (digital titrator made by Hach). The results are subsequently speciated (see below) to obtain bicarbonate and carbonate concentrations. Spectrophotometry using field portable units was used to measure dissolved oxygen, nitrate, nitrite, total ammonia, ferrous iron, total sulfide, and dissolved silica (Hach spectrophotometers and reagents). All of these chemical analyses are time sensitive, so our protocol is to complete them as soon as possible after sample collection. However, we have established that some tests, like ferrous iron, are also strongly temperature dependent. In most cases we use filtered samples that are sufficiently cool after the filtration process. In other cases where filtering would compromise the sample (dissolved oxygen, total sulfide) we have adopted protocols that minimize uncertainty.

Samples for major ions were filtered in the field through a series of 0.8 μ m and 0.2 μ m filters (such as Supor® filters made of hydrophilic polyethersulfone, Pall Scientific) and collected in 60 mL polypropylene bottles that are acid-washed, cleaned, and oven dried in the lab before leaving for the field. As quickly as possible after returning from

the field, major cation (Na⁺, K⁺, Ca⁺², Mg⁺²) and anion (sulfate⁻², Cl⁻, Br⁻, F⁻) concentrations were measured in the laboratory using ion chromatography (anions: Dionex IonPac AS11 Analytical and IonPac AG11 Guard columns; cations: Dionex IonPac CS12A Analytical and IonPac SG11 Guard columns; conductivity detection).

The continuous supply of gas that bubbles from Obsidian Pool permits collecting gas samples in Giggenbach bottles, which are 250 mL glass vials with valves into which known amounts of concentrated NaOH solutions are added before evacuation (Giggenbach 1975; Giggenbach and Goguel 1989; Giggenbach et al. 2001). Using established protocols, funnels and hoses are employed to trap the gas emanating from the hot spring source and deliver it to the Giggenbach bottle. Reactive gases, such as CO₂ and H₂S, which combine to account for the majority of the gas compositions at Yellowstone, dissolve into the caustic solution in the Giggenbach bottles. This allows the less reactive and less abundant gases (H₂, N₂, O₂, CO, CH₄, Ar, He, etc.) to accumulate in the headspace. It is not unusual to be able to store 10 to 15 L of gas in a Giggenbach bottle because the vast majority of the gas goes into solution. As a consequence, the minor and trace gases, which would be present at or below detection limits in their dissolved form, are concentrated in the headspace of the Giggenbach bottle, which facilitates accurate quantification of their mole fractions. Analysis of the headspace is accomplished with gas chromatography using thermal conductivity and flame ionization detectors. The dissolved gases (CO₂ and H₂S) are quantified with established wet chemical methods (Giggenbach and Goguel 1989). Our samples were analyzed in the lab of Tobias Fischer at the University of New Mexico, and results for Obsidian Pool gas samples are listed in **Table 2**.

6.0 CALCULATION OF DISEQUILIBRIA

The analytical field and laboratory data summarized in **Tables 1 and 2** permit analysis of the state of disequilibria for dozens of coupled oxidation-reduction reactions that are potential sources of energy for microbial metabolism in Obsidian Pool. There are two factors that affect the calculation of thermodynamic activities from measured concentrations—chemical speciation, and ionic strength effects. Chemical speciation is evaluated by taking explicit account of all gas solubility, acid dissociation, base protonation, and ion-pair equilibria in the aqueous phase, and determining how each of the elements or compounds of interest is distributed among the various possible aqueous forms (Krauskopf and Bird 1995; Zhu and Anderson 2002). We assume that magmatic gases and hot spring fluids obey Henry's law and reach equilibrium with respect to gas solubility reactions (Shock et al. 1989; Plyasunov and Shock 2003). Ionic strength calculations require major ion abundances and are used to evaluate activity coefficients using an extended form of the Debye-Hückel equation (see Amend and Shock 2001 for a summary related to microbial metabolism). We currently use a version of the EQ3/6 computer program to conduct these calculations (Wolery and Jarek 2003), with a customized database of equilibrium constants derived from our ongoing theoretical research (Shock et al. 1997; Sverjensky et al. 1997; Plyasunov and Shock 2001).

7.0 ENERGY STRUCTURE AT OBSIDIAN POOL

The case was made above for thinking of Obsidian Pool as a natural chemostat for the hydrogen oxidation reaction. Does

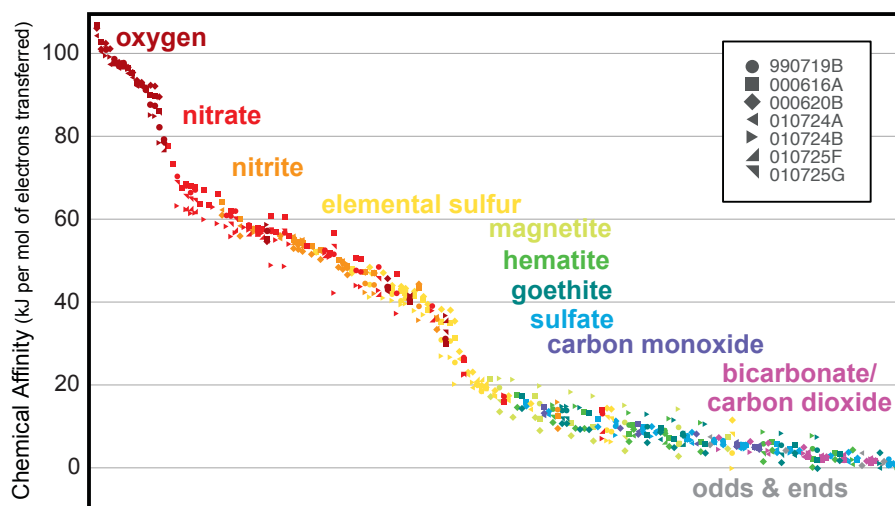


Figure 3. Compilation of chemical affinities (in kJ per mol of electrons transferred) for 182 potential metabolic energy sources from greatest (left) to least (right) in Obsidian Pool. Corresponding chemical reactions are identified and correlated to this diagram in the **Appendix** (page 12). Affinities, calculated with analytical data in **Tables 1 and 2**, together with equilibrium constants for each reaction, are color-coded by oxidant (electron acceptor) using symbols that correspond to the samples from the locations shown in **Figure 1**. The scatter of points for a single reaction reflects the natural variation of the hot spring system. Note that potential metabolic energy sources in which oxygen is the electron acceptor would tend to yield the greatest amounts of energy, followed by those involving nitrate, nitrite, sulfur and so on.

Obsidian Pool also act like a natural chemostat for other energy-yielding reactions? If so, how does the amount of energy from hydrogen oxidation compare to other energy-yielding chemical reactions? One way of contrasting the relative amounts of energy from redox reactions in which different numbers of electrons are involved is to make comparisons in terms of the chemical affinity per mole of electrons transferred, because microbial metabolism is based on electron transfer. Comparisons of this type are shown in **Figure 3** for all of the 182 energy-yielding redox reactions in Obsidian Pool that involve combinations of H_2 , O_2 , H_2O , H^+ , CO_2 (or HCO_3^-), CO , CH_4 , NO_3^- , NO_2^- , NH_4^+ , H_2S , SO_4^{2-} , Fe^{2+} , pyrite (FeS_2), sulfur, magnetite (Fe_3O_4), hematite (Fe_2O_3), and goethite ($FeOOH$). Each reaction is identified and correlated to this figure in the list in the **Appendix**, pp. 106-109. Because more positive values of chemical affinity correspond to greater potential energy sources, those reactions that occur toward the left of **Figure 3** yield the greatest amount of energy in Obsidian Pool (per electron transferred).

Note that the results shown in **Figure 3** are derived from several measurements over three field seasons. The natural variability is indicated by the scatter of data points in **Figure 3** and quantified as a standard deviation (corresponding to a 90% confidence interval) in the **Appendix**. The clustering of symbols for each reaction in **Figure 3** underlines the status of Obsidian Pool as a natural chemostat.

The results in **Figure 3** provide the first comprehensive view of the distribution of energy supplies from chemical reactions in a hot spring ecosystem. Several trends in the data prompt discussion. The group of reactions that supplies the greatest amounts of energy involves O_2 as the oxidant or electron acceptor. Although there is some mixing of oxidants among the ranked reactions, nitrate reduction reactions (in which nitrate is the electron acceptor) as a group are the next most abundant sources of chemical energy. Continuing this coarse sorting, the remaining oxidants in general order of decreasing energy are nitrite, sulfur, ferric iron (magnetite, hematite, or goethite), sulfate, carbon monoxide, and carbon dioxide (or bicarbonate). As a result, there is considerable similarity between the order of decreasing energy supplies in this hot spring and the order of changing oxidants with depth in marine or lacustrine sediments (Froelich et al. 1979; Nealson 1997; Hartnett and Devol 2003). Unlike sediments, which act much like a closed system resulting in the vertical stratification of energy use, the hot spring is an open system and all energy sources exist in the same location simultaneously. Nevertheless, the same thermodynamic necessities drive the distribution of energy supplies in the open system and the vertical stratification of energy use in the closed system. The most dramatic offsets in the energy supply at Obsidian Pool occur at the transition from oxygen to nitrate, and from sulfur to ferric iron. These transitions are marked by differences of about 20 kJ per mole of electrons transferred and give the diagram a pair of steps in what is otherwise a remarkably smooth curve.

8.0 DISCUSSION AND IMPLICATIONS

Five of the potential metabolic energy sources shown in **Figure 3** can be directly related to known microorganisms or well-founded metabolisms for Obsidian Pool. Identification of individual potential metabolic energy sources should be

facilitated with the quantitative results shown in the **Appendix**. Hydrogen oxidation, which is a well-established metabolic strategy for Aquificales, is among the most energetically favorable reactions that could support metabolism in this analysis (99.3 ± 3.7 kJ/mol e^-). Likewise, sulfur oxidation, another metabolic strategy employed by Aquificales, yields a similar amount of energy (97.4 ± 0.9 kJ/mol e^-). It is not yet known which, if either, of these reactions supports the Aquificales identified in clone libraries from Obsidian Pool. Nevertheless, it might be expected that Aquificales are abundant members of the microbial community if they are using their conventional energy sources and are not faced with other obstacles such as nutrient limitation or competition.

In contrast, ferric iron reduction (represented here by goethite reacting with H_2) yields about an order of magnitude less energy (11.5 ± 7.5 kJ/mol e^-). *G. ferrireducens* uses a similar reaction involving poorly crystalline iron oxides as its energy source. The overall difference between goethite and the poorly crystalline solid is probably a trivial contribution to this energy analysis. If so, the reaction that *G. ferrireducens* uses in Obsidian Pool has the potential to supply such a small amount of energy per mole of electrons transferred that it raises questions about how such small energy sources can be harnessed for biosynthetic processes.

Reactions in which ferrous ions combine with oxygen to yield iron oxides (goethite, hematite, and magnetite) supply closely similar amounts of energy to one another (89.0 ± 5.4 kJ/mol e^- , 88.8 ± 5.4 kJ/mol e^- , and 84.4 ± 8.4 kJ/mol e^- , respectively). These reactions yield about seven times as much energy as iron reduction. When grown in the lab, cultures of *G. ferrireducens* contain magnetite (Kashefi et al. 2002), and concentrations of Fe^{+2} change during the course of microbial growth. It may be worth investigating the enzymatic machinery of this organism to see if it is gaining energy from this reaction, which is far more favorable than iron reduction in Obsidian Pool.

Finally, sulfate reduction (with hydrogen as electron donor, 6.6 ± 2.7 kJ/mol e^-) is the least favorable of the reactions previously known or suspected to support life in Obsidian Pool. It is probable that sulfate reduction coupled to organic compound oxidation may yield more energy, but testing this

hypothesis will require analysis of organic compounds in hot spring samples (research we have recently begun; Cox et al. 2004; Windman et al. 2004). In any event, sulfate as an electron acceptor provides a feeble amount of energy compared to other reactants. Switching to reactions in which organic compounds replace hydrogen is not likely to cause a change in the overall ranking of electron acceptors as energy sources. In other words, oxidation of an organic compound with dissolved O_2 or nitrate should yield more energy per mole of electrons transferred than oxidizing the same organic compound with ferric iron or sulfate.

Some insight into the effects of geochemical composition on the availability of energy as well as the variability of energy structure in hydrothermal ecosystems can be gained by comparing the results reported here with those of Amend et al. (2003) for shallow submarine systems at Vulcano Island, Italy. In both cases, reactions with O_2 as the electron acceptor yield large amounts of energy. However, at Vulcano the coupling of iron reduction with methane or sulfide oxidation can yield more energy than some of the reactions involving O_2 .

One should keep in mind that the energy analysis presented here is based on gas and near-surface water samples from Obsidian Pool, and may not reflect the abundance or ranking of energy in the hot spring sediments or deeper in the hydrothermal system. In such environments we expect that the concentration of dissolved O_2 will decrease dramatically, which means that reactions involving O_2 as an electron acceptor will no longer yield the greatest amount of energy. Nitrate reduction may then be the top energy source, perhaps explaining the presence of strains in the clone libraries that plot with *Pyrobaculum* in phylogenetic analyses. In addition, care must be taken when comparing details of the ranking shown in **Figure 3** and the **Appendix** with any of the phylogenies determined for different samples collected at different times. There may have been changes in the hot spring composition, and surface water samples may not correlate directly with the compositions of microenvironments where individual microbial communities exist. Nevertheless, the analysis presented here reveals the overall energetic structure of a hydrothermal ecosystem, and the same methodologies

can be used in conjunction with sampling for phylogenetic analysis, or to improve the potential for isolating organisms by generating enrichment media based on the compositions of hot springs and thermodynamic calculations (Meyer-Dombard 2004).

The information in **Figure 3** is complementary to microbial community data obtained from clone libraries. On the one hand, clone libraries provide an inventory of organisms present in a natural system, as well as phylogenetic trees of their relatedness, but no direct information about their metabolism or physiology. On the other hand, the distribution of potential metabolic energy supplies is an inventory of the disequilibria that can support life in a natural system, but contains no direct evidence that life is using any of the reactions. In the case of Obsidian Pool, where photosynthesis is absent, it is a near certainty that all of the organisms revealed by the clone libraries are taking advantage of one or another of the disequilibria shown in **Figure 3** and ranked in the **Appendix**, either as their primary energy source or as electron donors or acceptors in reactions involving organic compounds. These two keys, together with continued attempts to obtain individual specimens in pure culture, will allow us to unlock the mysteries of microbial activity and community structure in hot spring ecosystems like Obsidian Pool.

ACKNOWLEDGMENTS

The results described above would not be possible without the efforts of many researchers who have joined us in expeditions to Yellowstone. In particular we wish to thank Bob Osburn for his exquisite maps composed during our expeditions in 1999–2001 (Figure 1 contains only a small fragment). Since 1999, Maggie Osburn, Beth Martin, Nathan Schnebly, Mike Singleton, Peter Schultzeiss, Mitch Schulte, Karyn Rogers, Todd Windman, Jeff Harvig, Alysia Cox, Andrew Dombard, Barb Winston, Rachel Lindvall, Sarah Strauss, Panjai Prapaipong, Bill Winston, Kelly Hermanson, Callen Hyland, Tom Neiderberger, Colin Enssle, Samantha Fernandes, Larry Marcus, and Gavin Chanall helped with sampling, spectrophotometry, mapping, and other measurements in the field. Natalya Zolotova

supervised the collection of data by ion chromatography, Tobias Fischer, Martine Simoes, Bethany Burnett, Eileen Dunn, Florian Schwandner, and Tom McCollom assisted with gas sampling. Special thanks to Tobias Fischer for providing analytical data for the gas samples, and access to his laboratory. We are grateful for the efforts of Christie Hendrix in the Resource Office at Yellowstone and other members of the National Park Service for their help with permits, logistics, and access to sampling locations. Finally, we want to thank Anna-Louise Reysenbach for introducing us, in person, to Obsidian Pool.

REFERENCES

- Amend, J.P., and E.L. Shock. 2001. Energetics of overall metabolic reactions of thermophilic and hyperthermophilic Archaea and Bacteria. *FEMS Microbiol Rev* 25:175-243.
- Amend, J.P., K.L. Rogers, E.L. Shock, S. Gurrieri, and S. Inguaggiato. 2003. Energetics of chemolithoautotrophy in the hydrothermal system of Vulcano island, southern Italy. *Geobiology* 1:37-58.
- Barns, S.M., C.F. Delwiche, J.D. Palmer, and N.R. Pace. 1996. Perspectives on archaeal diversity, thermophily and monophyly from environmental rRNA sequences. *Proc Natl Acad Sci* 93:9188-93.
- Barns, S.M., R.E. Fundyga, M.W. Jeffries, and N.R. Pace. 1994. Remarkable Archaeal Diversity Detected in a Yellowstone-National-Park Hot-Spring Environment. *Proc Natl Acad Sci* 91:1609-13.
- Brock, T.D. 1978. *Thermophilic Microorganisms and Life at High Temperatures*. New York: Springer-Verlag.
- Burggraf, S., P. Heyder, and N. Eis. 1997. A pivotal Archaea group. *Nature* 385:780.
- Burggraf, S., R. Huber, T. Mayer, P. Rosnagel, and R. Rachel. 2001. Isolation of hyperthermophilic Archaea previously detected by sequencing rDNA directly from the environment. In *Thermophiles: Biodiversity, Ecology, and Evolution* ed. A.-L. Reysenbach, M. Voytek, and R. Mancinelli, 93-101. New York: Kluwer Academic/Plenum Publishers.
- Christiansen, R.L. 2001. The Quaternary and Pliocene Yellowstone Plateau Volcanic Field of Wyoming, Idaho, and Montana. *US Geol Surv Prof Pap* 729-G.
- Cox, A.D., and E.L. Shock. 2003. Limits of microbial photosynthesis in hot spring ecosystems. Abstract B41D-0927. *EOS Trans AGU* 84:F309-10.
- Cox, J.S., M.E. Holland, and E.L. Shock. 2004. Dissolved free amino acids in hydrothermal springs at Yellowstone National Park, U.S.A. Abstract B21B-0888. *EOS Trans AGU* 85.
- Fishbain, S., J.G. Dillon, H.L. Gough, and D.A. Stahl. 2003. Linkage of high rates of sulfate reduction in Yellowstone hot springs to unique sequence types in the dissimilatory sulfate respiration pathway. *Appl Environ Microbiol* 69:3663-7.
- Froelich, P.N., et al. 1979. Early oxidation of organic matter in pelagic sediments of the equatorial atlantic: suboxic diagenesis. *Geochim Cosmochim Acta* 43:1075-90.
- Giggenbach, W.F. 1975. A simple method for the collection and analysis of volcanic gas samples. *Bull Volcanol* 39:132-45.
- Giggenbach, W.F., and R.L. Goguel. 1989. *Collection and Analysis of Geothermal and Volcanic Water and Gas Discharges*. Chemical Division Report. Department of Scientific and Industrial Research. CD 2401.
- Giggenbach, W.F., D. Tedesco, Y. Sulistiyo, A. Caprai, R. Cioni, F. Favara, T.P. Fischer, J.-I. Hirabayashi, M. Korzhinsky, M. Martini, I. Menyailov, and H. Shinohara. 2001. Evaluation of results from the fourth and fifth IAVCEI field workshop on volcanic gases, Volcano island, Italy and Java, Indonesia. *J Volcanol Geotherm Res* 108:157-72.
- Graber, J.R., J. Kirshtein, M. Speck, and A.-L. Reysenbach. 2001. Community structure along a thermal gradient in a stream near Obsidian Pool, Yellowstone National Park. In *Thermophiles: Biodiversity, Ecology, and Evolution* ed. A.-L. Reysenbach, M. Voytek, and R. Mancinelli, 81-91. New York: Kluwer Academic/Plenum Publishers.
- Hartnett, H.E., and A.H. Devol. 2003. Role of a strong oxygen-deficient zone in the preservation and degradation of organic matter: A carbon budget for the continental margins of northwest Mexico and Washington state. *Geochim Cosmochim Acta* 67:247-64.
- Huber, R., S. Burggraf, T. Mayer, S.M. Barns, P. Rosnagel, and K.O. Stetter. 1995. Isolation of a hyperthermophilic archeum predicted by in situ RNA analysis. *Nature* 376:57-8.
- Huber, R., D. Dyba, H. Huber, S. Burggraf, and R. Rachel. 1998. Sulfur-inhibited *Thermosphaera aggregans* sp. nov., a new genus of hyperthermophilic archaea isolated after its prediction from environmentally derived 16S rRNA sequences. *Int J Syst Bacteriol* 48:31-8.
- Hugenholtz, P., C. Pituille, K.L. Hershberger, and N.R. Pace. 1998. Novel division level bacterial diversity in a Yellowstone hot spring. *J Bacteriol* 180:366-76.
- Kashefi, K., D.E. Holmes, A.-L. Reysenbach, and D.R. Lovley. 2002. Use of Fe(III) as an electron acceptor to recover previously uncultured hyperthermophiles: Isolation and characterization of *Geothermobacterium ferrireducens* gen. nov., sp nov. *Appl Environ Microbiol* 68:1735-42.

- Krauskopf, K.B., and D.K. Bird. 1995. *Introduction to Geochemistry*, 3rd ed. New York: McGraw Hill.
- Meyer-Dombard, D.R. 2004. Geochemical Constraints on Microbial Diversity of Hydrothermal Ecosystems in Yellowstone National Park. PhD Thesis, Washington University.
- Meyer-Dombard, D.R., E.L. Shock, and J.P. Amend. Submitted. Thermophilic communities in three geochemically distinct geothermal ecosystems, Yellowstone National Park, USA. *Geobiology*.
- Nealson, K.H. 1997. Sediment bacteria: Who's there, what are they doing, and what's new? *Ann Rev Earth Planet Sci* 25:403-34.
- Plyasunov, A.V., and E.L. Shock. 2001. Correlation strategy for determining the parameters of the revised Helgeson-Kirkham-Flowers model for aqueous nonelectrolytes. *Geochim Cosmochim Acta* 65:3879-3900.
- Plyasunov, A.V., and E.L. Shock. 2003. Prediction of the vapor-liquid distribution constants for volatile nonelectrolytes in H₂O up to the critical temperature of water. *Geochim Cosmochim Acta* 67:4981-5009.
- Reysenbach, A.-L., and E.L. Shock. 2002 Merging genomes with geochemistry in hydrothermal ecosystems. *Science* 296:1077-82.
- Roychoudhury, A.N. 2004. Sulfate respiration in extreme environments: A kinetic study. *Geomicrobiol J* 21:33-43.
- Setchell, W.A. 1903. The upper temperature limits of life. *Science* 17:934-7.
- Shock, E.L., D.C. Sassani, M. Willis, and D.A. Sverjensky. 1997. Inorganic species in geologic fluids: Correlations among standard molal thermodynamic properties of aqueous ions and hydroxide complexes. *Geochim Cosmochim Acta* 61:907-50.
- Shock, E.L., H.C. Helgeson, and D.A. Sverjensky. 1989. Calculation of the thermodynamic and transport properties of aqueous species at high pressures and temperatures: Standard partial molal properties of inorganic neutral species. *Geochim Cosmochim Acta* 53:2157-83.
- Sverjensky, D.A., E.L. Shock, and H.C. Helgeson. 1997. Prediction of the thermodynamic properties of aqueous metal complexes to 1000°C and 5 kb. *Geochim Cosmochim Acta* 61:1359-1412.
- Werner, C., and S.L. Brantley. 2000. CO₂ emissions related to the Yellowstone volcanic system 2. Statistical sampling, total degassing, and transport mechanisms. *J Geophys Res* 105(B5):10831-46.
- Windmann, T.O., N. Zolotova, and E. Shock. 2004. Organic acids as heterotrophic energy sources in hydrothermal systems. Abstract B21B-0892. *EOS Trans AGU* 85.
- Wolery, T.W., and R.L. Jarek. 2003. *Software User's Manual EQ3/6, Version 8.0*. Software Document Number 10813-UM-8.0-00. U.S. Department of Energy, Office of Civilian Radioactive Waste Management.
- Zhu, C., and G. Anderson. 2002. *Environmental Applications of Geochemical Modeling*. Cambridge University Press.

APPENDIX

The depiction of chemical affinities for Obsidian Pool in **Figure 3** allows an overall view of the energy structure in this hydrothermal ecosystem, but does not permit identification of individual potential metabolic energy sources. The figure included in this appendix shows the same color-coded information as **Figure 3**, but also identifies each of the 182 reactions that serve as potential metabolic energy sources, and gives the average and standard deviation of each chemical affinity. The number in brackets after each reaction gives the number of electrons transferred in the reaction.

Geochemical Reaction

potential metabolic energy sources

| |
|--|
| CO(g) + 1/2 O ₂ (aq) + H ₂ O → HCO ₃ ⁻ + H ⁺ [2] |
| CO(g) + 1/2 O ₂ (aq) → CO ₂ (g) [2] |
| 2H ₂ S(aq) + Fe ⁺² + 1/2 O ₂ (aq) → PYRITE + 2H ⁺ + H ₂ O [2] |
| 2H ₂ (g) + O ₂ (aq) → 2H ₂ O [4] |
| 2MAGNETITE + 1/2 O ₂ (aq) + 3H ₂ O → 6GOETHITE [2] |
| SULFUR + 3/2 O ₂ (aq) + H ₂ O → SO ₄ ⁻² + 2H ⁺ [6] |
| 2MAGNETITE + 1/2 O ₂ (aq) → 3HEMATITE [2] |
| CH ₄ (g) + 2O ₂ (aq) → HCO ₃ ⁻ + H ⁺ + H ₂ O [8] |
| CH ₄ (g) + 2O ₂ (aq) → CO ₂ (g) + 2H ₂ O [8] |
| CH ₄ (g) + 3/2 O ₂ (aq) → CO(g) + 2H ₂ O [6] |
| H ₂ S(aq) + 2O ₂ (aq) → SO ₄ ⁻² + 2H ⁺ [8] |
| PYRITE + 7/2 O ₂ (aq) + H ₂ O → 2SO ₄ ⁻² + Fe ⁺² + 2H ⁺ [14] |
| Fe ⁺² + 1/4 O ₂ (aq) + 3/2 H ₂ O → GOETHITE + 2H ⁺ [1] |
| 2Fe ⁺² + 1/2 O ₂ (aq) + 2H ₂ O → HEMATITE + 4H ⁺ [2] |

Chemical Affinity (kJ per mol of electrons transferred)

| Average ± 2 sd | 0 | 20 | 40 | 60 | 80 | 100 |
|----------------|---|----|----|----|----|-----|
| 105.9 ± 2.6 | | | | | | |
| 101.5 ± 2.4 | | | | | | |
| 101.1 ± 2.4 | | | | | | |
| 99.3 ± 3.7 | | | | | | |
| 98.1 ± 0.9 | | | | | | |
| 97.4 ± 0.9 | | | | | | |
| 97.3 ± 0.9 | | | | | | |
| 96.2 ± 1.2 | | | | | | |
| 95.1 ± 1.1 | | | | | | |
| 92.9 ± 1.3 | | | | | | |
| 92.6 ± 0.8 | | | | | | |
| 91.6 ± 0.7 | | | | | | |
| 89.0 ± 5.4 | | | | | | |
| 88.8 ± 5.4 | | | | | | |

CONTINUED, NEXT PAGE

Geochemical Reaction

potential metabolic energy sources

Chemical Affinity (kJ per mol of electrons transferred)

Average ± 2 sd

| | | 0 | 20 | 40 | 60 | 80 | 100 |
|--|-------------|---|----|----|----|----|-----|
| | | | | | | | |
| 3Fe ²⁺ + 1/2 O ₂ (aq) + 3H ₂ O → MAGNETITE + 6H ⁺ [2] | 84.4 ± 8.4 | | | | | | → |
| H ₂ S(aq) + 1/2 O ₂ (aq) → SULFUR + H ₂ O [2] | 78.3 ± 1.8 | | | | | | → |
| CO(g) + NO ₃ ⁻ + H ₂ O → HCO ₃ ⁻ + NO ₂ ⁻ + H ⁺ [2] | 77.5 ± n/a | | | | | | → |
| CO(g) + NO ₃ ⁻ → CO ₂ (g) + NO ₂ ⁻ [2] | 73.4 ± n/a | | | | | | → |
| 2H ₂ S(aq) + NO ₃ ⁻ + Fe ²⁺ → PYRITE + NO ₂ ⁻ + 2H ⁺ + H ₂ O [2] | 67.4 ± 7.6 | | | | | | → |
| 4CO(g) + NO ₃ ⁻ + 5H ₂ O → 4HCO ₃ ⁻ + NH ₄ ⁺ + 2H ⁺ [8] | 67.4 ± n/a | | | | | | → |
| 2MAGNETITE + NO ₃ ⁻ + 3H ₂ O → 6GOETHITE + NO ₂ ⁻ [2] | 65.3 ± 5.8 | | | | | | → |
| SULFUR + 3NO ₃ ⁻ + H ₂ O → SO ₄ ²⁻ + 3NO ₂ ⁻ + 2H ⁺ [6] | 64.5 ± 5.6 | | | | | | → |
| 2MAGNETITE + NO ₃ ⁻ → 3HEMATITE + NO ₂ ⁻ [2] | 64.4 ± 5.8 | | | | | | → |
| CH ₄ (g) + 3NO ₃ ⁻ → CO(g) + 3NO ₂ ⁻ + 2H ₂ O [6] | 63.4 ± n/a | | | | | | → |
| CH ₄ (g) + 4NO ₃ ⁻ → HCO ₃ ⁻ + 4NO ₂ ⁻ + H ⁺ + H ₂ O [8] | 63.4 ± 10.1 | | | | | | → |
| 4CO(g) + NO ₃ ⁻ + 2H ⁺ + H ₂ O → 4CO ₂ (g) + NH ₄ ⁺ [8] | 63.2 ± n/a | | | | | | → |
| H ₂ (g) + NO ₃ ⁻ → NO ₂ ⁻ + H ₂ O [2] | 62.8 ± n/a | | | | | | → |
| CH ₄ (g) + 4NO ₃ ⁻ → CO ₂ (g) + 4NO ₂ ⁻ + 2H ₂ O [8] | 62.4 ± 10.0 | | | | | | → |
| 3CO(g) + NO ₂ ⁻ + 4H ₂ O → 3HCO ₃ ⁻ + NH ₄ ⁺ + H ⁺ [6] | 62.3 ± 3.2 | | | | | | → |
| 8H ₂ S(aq) + NO ₃ ⁻ + 4Fe ²⁺ → 4PYRITE + NH ₄ ⁺ + 6H ⁺ + 3H ₂ O [8] | 59.4 ± 3.7 | | | | | | → |
| PYRITE + 7NO ₃ ⁻ + H ₂ O → Fe ²⁺ + 2SO ₄ ²⁻ + 7NO ₂ ⁻ + 2H ⁺ [14] | 59.2 ± 5.4 | | | | | | → |
| H ₂ S(aq) + 4NO ₃ ⁻ → SO ₄ ²⁻ + 4NO ₂ ⁻ + 2H ⁺ [8] | 58.9 ± 4.9 | | | | | | → |
| 3CO(g) + NO ₂ ⁻ + 2H ⁺ + H ₂ O → 3CO ₂ (g) + NH ₄ ⁺ [6] | 57.9 ± 4.2 | | | | | | → |
| 4H ₂ (g) + NO ₃ ⁻ + 2H ⁺ → NH ₄ ⁺ + 3H ₂ O [8] | 57.9 ± n/a | | | | | | → |
| 8MAGNETITE + NO ₃ ⁻ + 2H ⁺ + 13H ₂ O → 24GOETHITE + NH ₄ ⁺ [8] | 57.5 ± 2.1 | | | | | | → |
| 6H ₂ S(aq) + NO ₂ ⁻ + 3Fe ²⁺ → 3PYRITE + NH ₄ ⁺ + 4H ⁺ + 2H ₂ O [6] | 57.1 ± 1.1 | | | | | | → |
| 4SULFUR + 3NO ₃ ⁻ + 7H ₂ O → 4SO ₄ ²⁻ + 3NH ₄ ⁺ + 2H ⁺ [24] | 56.8 ± 1.5 | | | | | | → |
| 8MAGNETITE + NO ₃ ⁻ + 2H ⁺ + H ₂ O → 12HEMATITE + NH ₄ ⁺ [8] | 56.7 ± 2.0 | | | | | | → |
| PYRITE + 2H ⁺ + 1/2 O ₂ (aq) → 2SULFUR + Fe ²⁺ + H ₂ O [2] | 56.0 ± 3.6 | | | | | | → |
| 2Fe ²⁺ + NO ₃ ⁻ + 3H ₂ O → 2GOETHITE + NO ₂ ⁻ + 4H ⁺ [2] | 55.9 ± 10.1 | | | | | | → |
| CH ₄ (g) + NO ₃ ⁻ + H ⁺ → HCO ₃ ⁻ + NH ₄ ⁺ [8] | 55.8 ± 2.7 | | | | | | → |
| 3H ₂ (g) + NO ₂ ⁻ + 2H ⁺ → NH ₄ ⁺ + 2H ₂ O [6] | 55.7 ± 1.0 | | | | | | → |
| 2Fe ²⁺ + NO ₃ ⁻ + 2H ₂ O → HEMATITE + NO ₂ ⁻ + 4H ⁺ [2] | 55.6 ± 10.1 | | | | | | → |
| CH ₄ (g) + NO ₃ ⁻ + 2H ⁺ → CO ₂ (g) + NH ₄ ⁺ + H ₂ O [8] | 54.8 ± 2.7 | | | | | | → |
| 6MAGNETITE + NO ₂ ⁻ + 2H ⁺ + 10H ₂ O → 18GOETHITE + NH ₄ ⁺ [6] | 54.7 ± 2.3 | | | | | | → |
| SULFUR + NO ₂ ⁻ + 2H ₂ O → SO ₄ ²⁻ + NH ₄ ⁺ [6] | 53.9 ± 1.5 | | | | | | → |
| 6MAGNETITE + NO ₂ ⁻ + 2H ⁺ + H ₂ O → 9HEMATITE + NH ₄ ⁺ [6] | 53.9 ± 2.2 | | | | | | → |
| 4CH ₄ (g) + 3NO ₃ ⁻ + 6H ⁺ → 4CO(g) + 3NH ₄ ⁺ + 5H ₂ O [24] | 53.3 ± n/a | | | | | | → |
| 3CH ₄ (g) + 4NO ₂ ⁻ + 5H ⁺ + H ₂ O → 3HCO ₃ ⁻ + 4NH ₄ ⁺ [24] | 52.7 ± 1.9 | | | | | | → |
| 2SULFUR + CO(g) + Fe ²⁺ + 2H ₂ O → PYRITE + HCO ₃ ⁻ + 3H ⁺ [2] | 51.8 ± 0.1 | | | | | | → |
| 3CH ₄ (g) + 4NO ₂ ⁻ + 8H ⁺ → 3CO ₂ (g) + 4NH ₄ ⁺ + 2H ₂ O [24] | 51.6 ± 2.2 | | | | | | → |
| H ₂ S(aq) + NO ₃ ⁻ + H ₂ O → SO ₄ ²⁻ + NH ₄ ⁺ [8] | 51.6 ± 1.4 | | | | | | → |
| 4PYRITE + 7NO ₃ ⁻ + 6H ⁺ + 11H ₂ O → 4Fe ²⁺ + 8SO ₄ ²⁻ + 7NH ₄ ⁺ [56] | 51.2 ± 1.1 | | | | | | → |
| 3Fe ²⁺ + NO ₃ ⁻ + 3H ₂ O → MAGNETITE + NO ₂ ⁻ + 6H ⁺ [2] | 50.8 ± 12.6 | | | | | | → |
| CH ₄ (g) + NO ₂ ⁻ + 2H ⁺ → CO(g) + NH ₄ ⁺ + H ₂ O [6] | 49.3 ± 2.0 | | | | | | → |
| 3H ₂ S(aq) + 4NO ₂ ⁻ + 2H ⁺ + 4H ₂ O → 3SO ₄ ²⁻ + 4NH ₄ ⁺ [24] | 49.1 ± 1.8 | | | | | | → |
| 3PYRITE + 7NO ₂ ⁻ + 8H ⁺ + 10H ₂ O → 3Fe ²⁺ + 6SO ₄ ²⁻ + 7NH ₄ ⁺ [42] | 47.9 ± 2.3 | | | | | | → |
| 2SULFUR + CO(g) + Fe ²⁺ + H ₂ O → PYRITE + CO ₂ (g) + 2H ⁺ [2] | 47.2 ± 1.4 | | | | | | → |
| 8Fe ²⁺ + NO ₃ ⁻ + 13H ₂ O → 8GOETHITE + NH ₄ ⁺ + 14H ⁺ [8] | 47.2 ± 6.6 | | | | | | → |
| 8Fe ²⁺ + NO ₃ ⁻ + 9H ₂ O → 4HEMATITE + NH ₄ ⁺ + 14H ⁺ [8] | 46.9 ± 6.7 | | | | | | → |
| 6Fe ²⁺ + NO ₂ ⁻ + 10H ₂ O → 6GOETHITE + NH ₄ ⁺ + 10H ⁺ [6] | 45.1 ± 4.7 | | | | | | → |
| SULFUR + H ₂ S(aq) + Fe ²⁺ → PYRITE + 2H ⁺ [1] | 44.9 ± 6.3 | | | | | | → |
| 6Fe ²⁺ + NO ₂ ⁻ + 7H ₂ O → 3HEMATITE + NH ₄ ⁺ + 10H ⁺ [6] | 44.8 ± 4.8 | | | | | | → |
| H ₂ S(aq) + NO ₃ ⁻ → SULFUR + NO ₂ ⁻ + H ₂ O [2] | 44.5 ± 6.1 | | | | | | → |
| 2SULFUR + H ₂ (g) + Fe ²⁺ → PYRITE + 2H ⁺ [2] | 43.8 ± 8.5 | | | | | | → |
| NH ₄ ⁺ + 3/2 O ₂ (aq) → NO ₂ ⁻ + 2H ⁺ + H ₂ O [6] | 43.5 ± 2.1 | | | | | | → |
| 2SULFUR + 2MAGNETITE + Fe ²⁺ + 4H ₂ O → PYRITE + 6GOETHITE + 2H ⁺ [2] | 42.3 ± 2.8 | | | | | | → |
| 12Fe ²⁺ + NO ₃ ⁻ + 13H ₂ O → 4MAGNETITE + NH ₄ ⁺ + 22H ⁺ [8] | 41.8 ± 9.5 | | | | | | → |

CONTINUED, NEXT PAGE

Geochemical Reaction

potential metabolic energy sources

Chemical Affinity (kJ per mol of electrons transferred)

| | Average ± 2 sd | 0 | 20 | 40 | 60 | 80 | 100 |
|---|----------------|---|----|----|----|----|-----|
| 7H ₂ (g) + 2SO ₄ ²⁻ + Fe ⁺² + 2H ⁺ → PYRITE + 8H ₂ O [14] | 8.3 ± 3.3 | | | | | | |
| 4CO(g) + SO ₄ ²⁻ + 2H ⁺ → 4CO ₂ (g) + H ₂ S(aq) [8] | 8.3 ± 0.7 | | | | | | |
| 6GOETHITE + CO(g) → 2MAGNETITE + HCO ₃ ⁻ + H ⁺ + 2H ₂ O [2] | 7.9 ± 2.8 | | | | | | |
| 2HEMATITE + 2H ₂ S(aq) → PYRITE + MAGNETITE + 2H ₂ O [2] | 7.7 ± 2.2 | | | | | | |
| 4HEMATITE + CH ₄ (g) + 15H ⁺ → HCO ₃ ⁻ + 8Fe ⁺² + 9H ₂ O [8] | 7.5 ± 7.0 | | | | | | |
| 8GOETHITE + CH ₄ (g) + 15H ⁺ → HCO ₃ ⁻ + 8Fe ⁺² + 13H ₂ O [8] | 7.3 ± 6.9 | | | | | | |
| PYRITE + 7MAGNETITE + 40H ⁺ → 2SO ₄ ²⁻ + 22Fe ⁺² + 20H ₂ O [14] | 7.2 ± 8.8 | | | | | | |
| 4GOETHITE + 2H ₂ S(aq) → PYRITE + MAGNETITE + 4H ₂ O [2] | 7.2 ± 2.1 | | | | | | |
| 14MAGNETITE + Fe ⁺² + 2SO ₄ ²⁻ + 2H ⁺ + 20H ₂ O → PYRITE + 42GOETHITE [14] | 6.7 ± 0.7 | | | | | | |
| 4H ₂ (g) + SO ₄ ²⁻ + 2H ⁺ → H ₂ S(aq) + 4H ₂ O [8] | 6.6 ± 2.7 | | | | | | |
| CO(g) + 3H ₂ (g) → CH ₄ (g) + H ₂ O [6] | 6.4 ± 3.4 | | | | | | |
| 4HEMATITE + CH ₄ (g) + 16H ⁺ → CO ₂ (g) + 8Fe ⁺² + 10H ₂ O [8] | 6.4 ± 7.2 | | | | | | |
| 8GOETHITE + CH ₄ (g) + 16H ⁺ → CO ₂ (g) + 8Fe ⁺² + 14H ₂ O [8] | 6.2 ± 7.2 | | | | | | |
| CO(g) + 2H ₂ O → H ₂ (g) + HCO ₃ ⁻ + H ⁺ [2] | 6.0 ± 2.7 | | | | | | |
| 14MAGNETITE + Fe ⁺² + 2SO ₄ ²⁻ + 2H ⁺ → PYRITE + 21HEMATITE + H ₂ O [14] | 5.9 ± 0.6 | | | | | | |
| CO ₂ (g) + 4Fe ⁺² + 8H ₂ S(aq) → 4PYRITE + CH ₄ (g) + 8H ⁺ + 2H ₂ O [8] | 5.7 ± 4.0 | | | | | | |
| 8MAGNETITE + SO ₄ ²⁻ + 2H ⁺ + 12H ₂ O → 24GOETHITE + H ₂ S(aq) [8] | 5.6 ± 0.8 | | | | | | |
| 3MAGNETITE + CH ₄ (g) + 18H ⁺ → CO(g) + 9Fe ⁺² + 11H ₂ O [6] | 5.4 ± 3.9 | | | | | | |
| SULFUR + 3Fe ⁺² + 4H ₂ O → MAGNETITE + H ₂ S(aq) + 6H ⁺ [2] | 5.3 ± 10.3 | | | | | | |
| 6MAGNETITE + CO(g) + 11H ₂ O → 18GOETHITE + CH ₄ (g) [6] | 5.1 ± 1.3 | | | | | | |
| 8MAGNETITE + SO ₄ ²⁻ + 2H ⁺ → 12HEMATITE + H ₂ S(aq) [8] | 4.7 ± 0.7 | | | | | | |
| 7CH ₄ (g) + 8SO ₄ ²⁻ + H ⁺ + 4Fe ⁺² → 4PYRITE + 7HCO ₃ ⁻ + 11H ₂ O [56] | 4.7 ± 1.0 | | | | | | |
| 4Fe ⁺² + HCO ₃ ⁻ + 8H ₂ S(aq) → 4PYRITE + CH ₄ (g) + 7H ⁺ + 3H ₂ O [8] | 4.6 ± 3.6 | | | | | | |
| SULFUR + CO(g) + 3H ₂ O → CH ₄ (g) + SO ₄ ²⁻ + 2H ⁺ [6] | 4.4 ± 0.3 | | | | | | |
| 6MAGNETITE + CO(g) + 2H ₂ O → 9HEMATITE + CH ₄ (g) [6] | 4.4 ± 1.1 | | | | | | |
| 4HEMATITE + H ₂ S(aq) + 14H ⁺ → SO ₄ ²⁻ + 8Fe ⁺² + 8H ₂ O [8] | 4.3 ± 6.2 | | | | | | |
| CO ₂ (g) + 4H ₂ (g) → CH ₄ (g) + 2H ₂ O [8] | 4.3 ± 2.6 | | | | | | |
| 3HEMATITE + CO(g) → 2MAGNETITE + CO ₂ (g) [2] | 4.2 ± 2.5 | | | | | | |
| 3CO(g) + SO ₄ ²⁻ + 2H ⁺ → SULFUR + 3CO ₂ (g) + H ₂ O [6] | 4.2 ± 2.2 | | | | | | |
| 8GOETHITE + H ₂ S(aq) + 14H ⁺ → SO ₄ ²⁻ + 8Fe ⁺² + 12H ₂ O [8] | 4.0 ± 6.2 | | | | | | |
| PYRITE + CO(g) + H ⁺ + 2H ₂ O → Fe ⁺² + HCO ₃ ⁻ + 2H ₂ S(aq) [2] | 3.7 ± n/a | | | | | | |
| 7CH ₄ (g) + 8SO ₄ ²⁻ + 8H ⁺ + 4Fe ⁺² → 4PYRITE + 7CO ₂ (g) + 18H ₂ O [56] | 3.6 ± 0.8 | | | | | | |
| 6GOETHITE + CO(g) → 2MAGNETITE + CO ₂ (g) + 3H ₂ O [2] | 3.5 ± 2.6 | | | | | | |
| CH ₄ (g) + SO ₄ ²⁻ + H ⁺ → HCO ₃ ⁻ + H ₂ S(aq) + H ₂ O [8] | 3.4 ± 0.5 | | | | | | |
| 4H ₂ (g) + HCO ₃ ⁻ + H ⁺ → CH ₄ (g) + 3H ₂ O [8] | 3.2 ± 2.3 | | | | | | |
| 8MAGNETITE + CO ₂ (g) + 14H ₂ O → 24GOETHITE + CH ₄ (g) [8] | 3.1 ± 1.2 | | | | | | |
| PYRITE + 7HEMATITE + 26H ⁺ → 2SO ₄ ²⁻ + 15Fe ⁺² + 13H ₂ O [14] | 2.8 ± 5.8 | | | | | | |
| PYRITE + 14GOETHITE + 26H ⁺ → 2SO ₄ ²⁻ + 15Fe ⁺² + 20H ₂ O [14] | 2.6 ± 5.8 | | | | | | |
| 8MAGNETITE + CO ₂ (g) + 2H ₂ O → 12HEMATITE + CH ₄ (g) [8] | 2.3 ± 1.0 | | | | | | |
| 4SULFUR + 3CO ₂ (g) + 10H ₂ O → 3CH ₄ (g) + 4SO ₄ ²⁻ + 8H ⁺ [24] | 2.3 ± 0.4 | | | | | | |
| CH ₄ (g) + SO ₄ ²⁻ + 2H ⁺ → CO ₂ (g) + H ₂ S(aq) + 2H ₂ O [8] | 2.3 ± 0.1 | | | | | | |
| 3HEMATITE + CH ₄ (g) + 12H ⁺ → CO(g) + 6Fe ⁺² + 8H ₂ O [6] | 2.3 ± 2.4 | | | | | | |
| 6GOETHITE + CH ₄ (g) + 12H ⁺ → CO(g) + 6Fe ⁺² + 11H ₂ O [6] | 2.0 ± 2.4 | | | | | | |
| 8MAGNETITE + HCO ₃ ⁻ + H ⁺ + 13H ₂ O → 24GOETHITE + CH ₄ (g) [8] | 2.0 ± 1.4 | | | | | | |
| 3H ₂ (g) + SO ₄ ²⁻ + 2H ⁺ → SULFUR + 4H ₂ O [6] | 1.9 ± 2.4 | | | | | | |
| 3HEMATITE + H ₂ (g) → 2MAGNETITE + H ₂ O [2] | 1.8 ± 3.5 | | | | | | |
| 7CH ₄ (g) + 6SO ₄ ²⁻ + 6H ⁺ + 3Fe ⁺² → 3PYRITE + 7CO(g) + 17H ₂ O [42] | 1.7 ± 0.5 | | | | | | |
| CO(g) + H ₂ O → CO ₂ (g) + H ₂ (g) [2] | 1.5 ± 4.4 | | | | | | |
| CO ₂ (g) + Fe ⁺² + 2H ₂ S(aq) → PYRITE + CO(g) + 2H ⁺ + H ₂ O [2] | 1.4 ± n/a | | | | | | |
| 8MAGNETITE + HCO ₃ ⁻ + H ⁺ + H ₂ O → 12HEMATITE + CH ₄ (g) [8] | 1.3 ± 1.2 | | | | | | |
| 4SULFUR + 3HCO ₃ ⁻ + 7H ₂ O → 3CH ₄ (g) + 4SO ₄ ²⁻ + 5H ⁺ [24] | 1.2 ± 0.3 | | | | | | |
| 6GOETHITE + H ₂ (g) → 2MAGNETITE + 4H ₂ O [2] | 1.0 ± 3.7 | | | | | | |
| 2H ₂ S(aq) + Fe ⁺² → PYRITE + H ₂ (g) + 2H ⁺ [2] | 0.8 ± 1.5 | | | | | | |
| 6MAGNETITE + SO ₄ ²⁻ + 2H ⁺ + 8H ₂ O → SULFUR + 18GOETHITE [6] | 0.8 ± 1.2 | | | | | | |
| 4CH ₄ (g) + 3SO ₄ ²⁻ + 6H ⁺ → 4CO(g) + 3H ₂ S(aq) + 8H ₂ O [24] | 0.3 ± 0.4 | | | | | | |
| SULFUR + 9HEMATITE + H ₂ O → 6MAGNETITE + SO ₄ ²⁻ + 2H ⁺ [6] | 0.1 ± 1.1 | | | | | | |

